

Investigation of the Optimal Position of Wind Sensors and Wind Turbines on A Building: A Computational Fluid Dynamics Study

Leon Chan*, Mohd Eqwan Bin Mohd Roslan and Hassan Bin Mohamed
Department of Mechanical Engineering, Universiti Tenaga Nasional, Kajang 43000,
Corresponding author, *e-mail: leonchan@uniten.edu.my

Abstract

Most numerical studies on flow over buildings simplify the geometry of the roof and assume that it is flat. This may lead to misrepresentation of the flow as the roof of actual buildings contains some sort of roughness. In this study, the flow over the administrative building of Universiti Tenaga Nasional is investigated for multidirectional flow conditions. The actual topology of the building is gridded and simulated using the steady-state Reynolds-averaged Navier-Stokes equation. Four points at the top of the building are identified and the wind statistics at these designated locations at three different heights are investigated. The optimal location with the highest average wind speed and consistent wind speeds for all wind angles is identified and is earmarked as a potential location to install the wind turbine.

Keywords: Wind Energy, Flow Over Buildings, Computational Fluid Dynamics

Copyright © 2017 Institute of Advanced Engineering and Science. All rights reserved.

1. Introduction

Malaysia voluntarily agreed to reduce its greenhouse gas (GHG) emissions intensity of GDP by 45% by 2030 compared to the baseline in 2005. The first 35% reduction is on an unconditional basis and the further 10% upon receiving climate finance, technology transfer and capacity building from developed countries [1]. Building-integrated renewable energy reduces reliance on conventional source of electricity without additional use of land space. One of the technologies available is roof-mounted wind turbine, which converts kinetic energy of wind surrounding the building into electricity. This method can be easily retrofitted to existing buildings. However, estimating the energy yield of a rooftop wind turbine is not trivial as the mean wind speed of the roof depends on the topology of the surroundings and also the shape of the roof of the building.

Conducting an experimental study is not only costly but also time consuming. Therefore, to better understand the flow physics over buildings, conducting computational fluid dynamics (CFD) is preferred as many test cases can be simulated to investigate the flow without requiring a specialised facility. Throughout the years, there has been many numerical studies conducted on flows over buildings. Heath et. al. investigated the flow over a pitched roof in isolation and also in arrays to replicate a typical residential area [2]. In another CFD study, Ledo et. al. simulated an array of buildings with three different basic roof shapes (flat roof, pitched roof and pyramidal roof). They found that the corners and edges of the roof are suitable for turbine installation [3]. However, at the edges, the flows is skewed due to the upward vertical flow of the walls of the building. Mertens argued that although skewed flow is beneficial for vertical axis wind turbines, high turbulence and separation bubble on the roof damages wind turbine and causes fatigue, resulting in power losses [4]. The effects of different roof shapes and wind directions on the flow of incoming wind have also been investigated by Abohela et. al. [5].

It is important to note that many of these studies [2], [3], [5]–[7] have simulated idealised roof shapes or a flat roof which might not be representative of the topology at the top of an actual building. The topology of the roof is often simplified as it is computationally expensive to capture the various small scale roughness on the roof. In this study, the flow over the administrative building (known as BA) of Universiti Tenaga Nasional (UNITEN) is investigated. In this feasibility study, the actual topology of the building has been simulated to accurately

model the flow and to determine the optimum location to install the wind sensors and wind turbine.

2. Computational Setup

The computational domain and the dimensions of the BA building is illustrated in figure 1. The dimensions of the building is obtained from the actual architectural drawings of the building. The x-axis represent the streamwise direction of the flow, y-axis denotes the spanwise direction and the z-axis denotes the wall-normal direction.

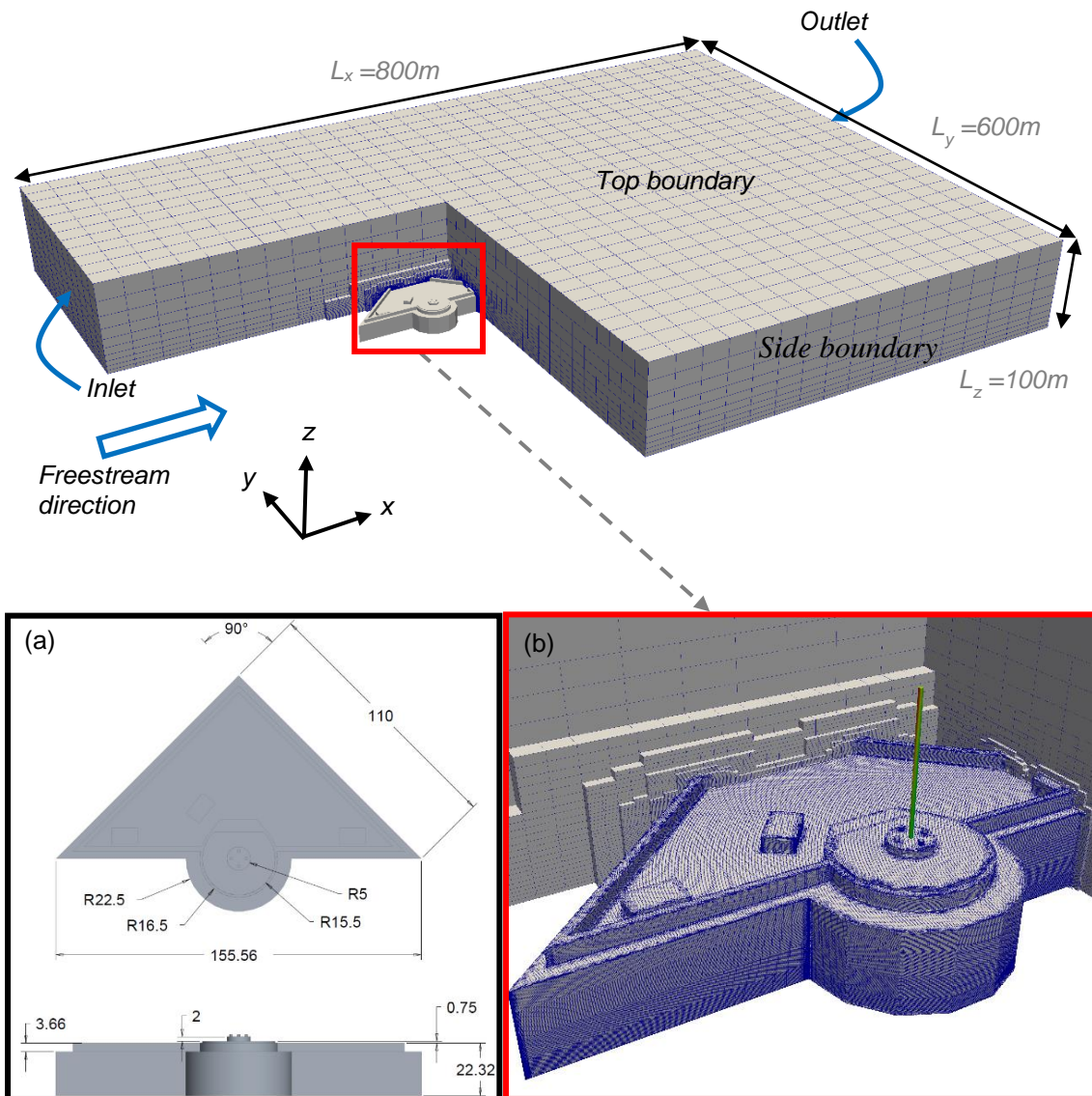


Figure 1: Computational mesh of the BA building with 0° wind angle. The centre of the building is located 300m from the inlet. The inset (a) shows the dimensions of the BA building in meters and (b) the mesh on the surface of the BA building. The vertical red line denotes the centre of the building/domain ($x=0m, y=0m$).

The no-slip, impermeable wall condition is applied to the bottom boundary and also to the walls of the BA building. For the top and side boundaries, a mirror boundary condition is

applied. The modified logarithmic velocity profile is used as the boundary condition for the inlet. This logarithmic profile is modified to include the effects of roughness caused by vegetation and buildings and follows the equation below

$$U_x(z) = U_r/\kappa \ln ((z-d)/z_0) \quad (1)$$

where U_x is the freestream velocity, U_r is the friction velocity, $\kappa=0.4$ is the Von Kármán constant, d is the zero-plane displacement height and z_0 is the momentum roughness length. The zero-plane displacement height $d = 0.7k$ and the momentum roughness length $z_0=0.1k$ where $k=5m$ is the mean building/vegetation height of the surroundings. This logarithmic profile has been used previously by [1,2]. The value of U_r is selected by fixing $U_x(z = 23m) = 2m/s$. The velocity is selected based on actual wind data collected which averaged around $2m/s$. The zero gradient boundary condition is applied to the outlet of the domain.

A large computational domain is used to ensure that the flow is not restricted by the computational boundaries. The mesh is stretched in the wall-normal direction with an expansion ratio of 1.19 and is equally spaced in the streamwise and the spanwise direction. The mesh in the vicinity of the BA building is locally refined to ensure that all of the topological features of the building (particularly the roof) is accurately captured (see inset of figure 1). To simulate the flow over the BA building at different angles, the geometry of the building is rotated and the computational domain is remeshed to ensure that the streamwise direction of the flow is always in the x -direction. The number of cells for each case ranges from 2.36-2.59 million. Increasing the number of cells to 7.96 million does not significantly change the drag and lift coefficients of the building (< 1% difference) and therefore indicates mesh independence. In these simulations, it is assumed that the ground is flat. This assumption is reasonable as the height variation of the undulating ground is small compared to the height of the building.

All simulations were conducted using the steady-state Reynolds-averaged Navier-Stokes equation with the standard Spalart-Allmaras turbulence model. The simpleFoam solver in OpenFOAM® version 2.1.1 was used to simulate the flow [9]. The gradient and diffusive terms were discretised using second-order central differencing scheme and the convective terms were discretised with the second-order upwind scheme. The kinematic viscosity of the fluid is $\nu = 1.5 \times 10^{-5} m^2/s$ which is of air at $20^\circ C$. Simulations were run until the lift and drag coefficients of the building converges (typically within 500-1000 iterations).

3. Results

Four locations on the roof of the BA building are identified as potential placements of the wind sensors and wind turbine. They are located at (x,y,z) coordinates Point 1: $(0,0,z)$, Point 2: $(30,20,z)$, Point 3: $(-30,20,z)$ and Point 4: $(0,45,z)$ (see figure 2(d)). The horizontal wind velocity magnitude ($|U_{xy}| = (U_x^2 + U_y^2)^{1/2}$) at these four locations are investigated at three different heights ($z = 23m, 25m$ and $27m$). Figure 2(a-c) illustrates the plot of the horizontal wind velocity magnitude for the four points at heights $z = 23m, 25m$ and $27m$ respectively. For point 1 at $z = 23m$ and $25m$, the velocity magnitude is set to be zero as the points are located within the building.

At a height of $23m$ (figure 2(a)), point 2 has the highest mean velocity. It also has the least number of wind angles which are below the mean (3 of 8 angles). On the contrary, point 4 has the lowest mean velocity. Despite having the lowest mean velocity, it has the highest minimum and maximum velocity compared to the other points. Wind speed magnitude for most wind angles (6 of 8 angles) is also lower than the mean velocity and has the largest standard deviation which is not a favourable location to place a wind turbine (see table 1).

Point 3 has the highest mean wind speed at $z = 25m$ while point 4 still has the lowest mean wind speed (figure 2(b)). It is interesting that point 3 now has a higher mean wind speed than point 2 although it appears to be surrounded by rectangular blocks. These obstacles actually channel the wind to the wind turbine and accelerate the flow. Point 2 has the lowest minimum and maximum wind speed at this height and would not be a good location to place wind turbine/measuring device as there is a large scatter in the data depending on the angle of the wind (as reflected in the high standard deviation in table 1).

Overall, the mean wind speed increases with height due to the logarithmic velocity profile which was used to model the atmospheric boundary layer. In addition, the higher the

placement of the wind sensors, the less likely it is being blocked by the structures on the roof and therefore does not reside within the turbulent wake of these structures. At $z = 27m$, point 1 has the highest average wind speed which is 32% larger than the average wind speed at point 4. This would then correspond to a significantly higher power output from the wind turbine.

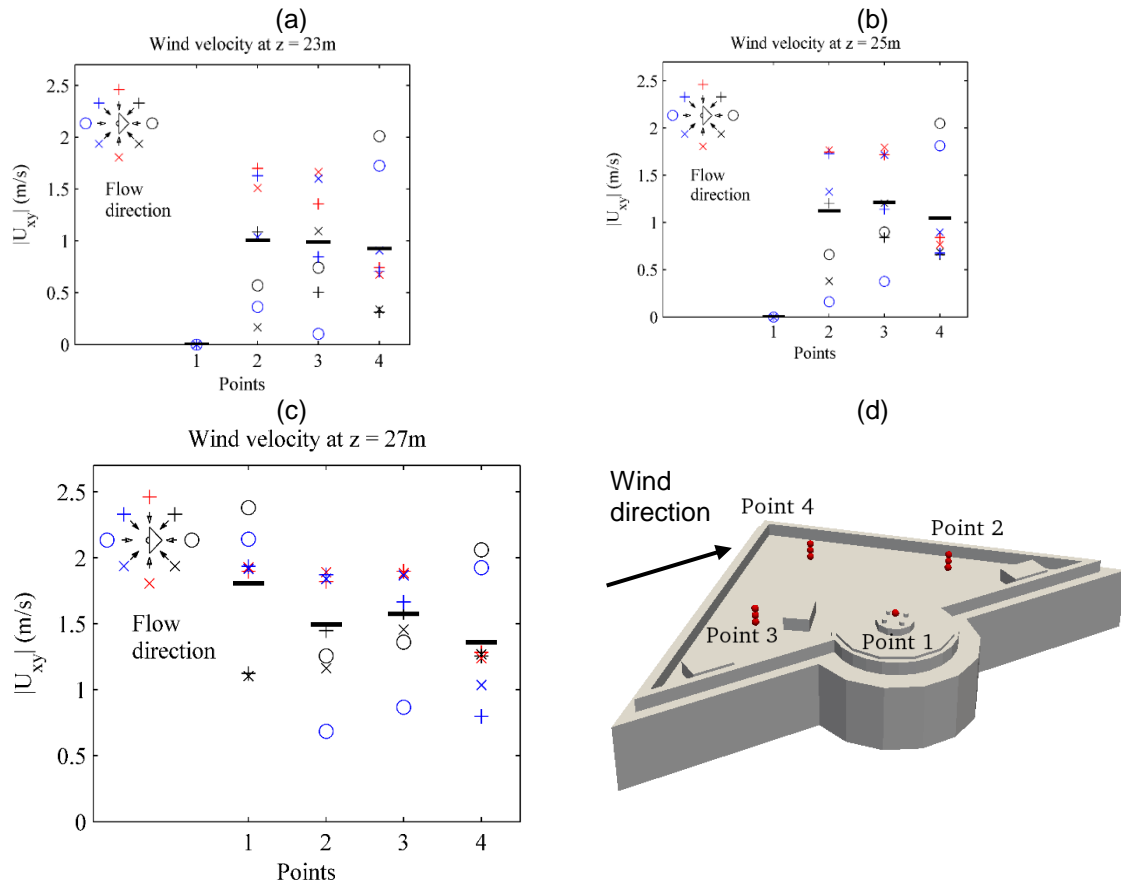


Figure 2: Plot of the horizontal wind speed magnitude $|U|$ at (a) $z = 23m$, (b) $z = 25m$ and (c) $z = 27m$. The black horizontal dashed lines represents the mean velocity. (d) Location of points 1, 2, 3 and 4 at 0° wind angle.

At points 1 and 4, the horizontal wind velocity magnitude is very large at wind angles 90° and 270° (see \circ and \circ symbols in figure 2). Looking at the volume rendering of the velocity magnitude around the BA building in figures 3(a,b), we see that the location of these points does not reside within the wake of the flow. On the other hand, points 2 and 3 have lower wind speeds at these angles as they are located within the turbulent wake of the flow.

The region of low speed wind is more significant at angle $\theta = 270^\circ$ (figure 3(b)) as observed by the strong green and yellow contours. At this wind angle, the flow resembles a flow over a bluff body. For angle $\theta = 90^\circ$ (figure 3(a)) the sharp edge of the building splits flow and channels the flow around the building rather than over the buildings. Therefore there is higher wind speed at the roof and a much smaller region of low wind speed at the sides of the building. Actual preliminary wind data collected from the BA building found that the direction of the wind typically occurs at an angle of 225° . Based on this information, point 3 will be the most suitable location at $z = 23m$ and $25m$ while point 1 will be the optimum location at $z = 27m$.

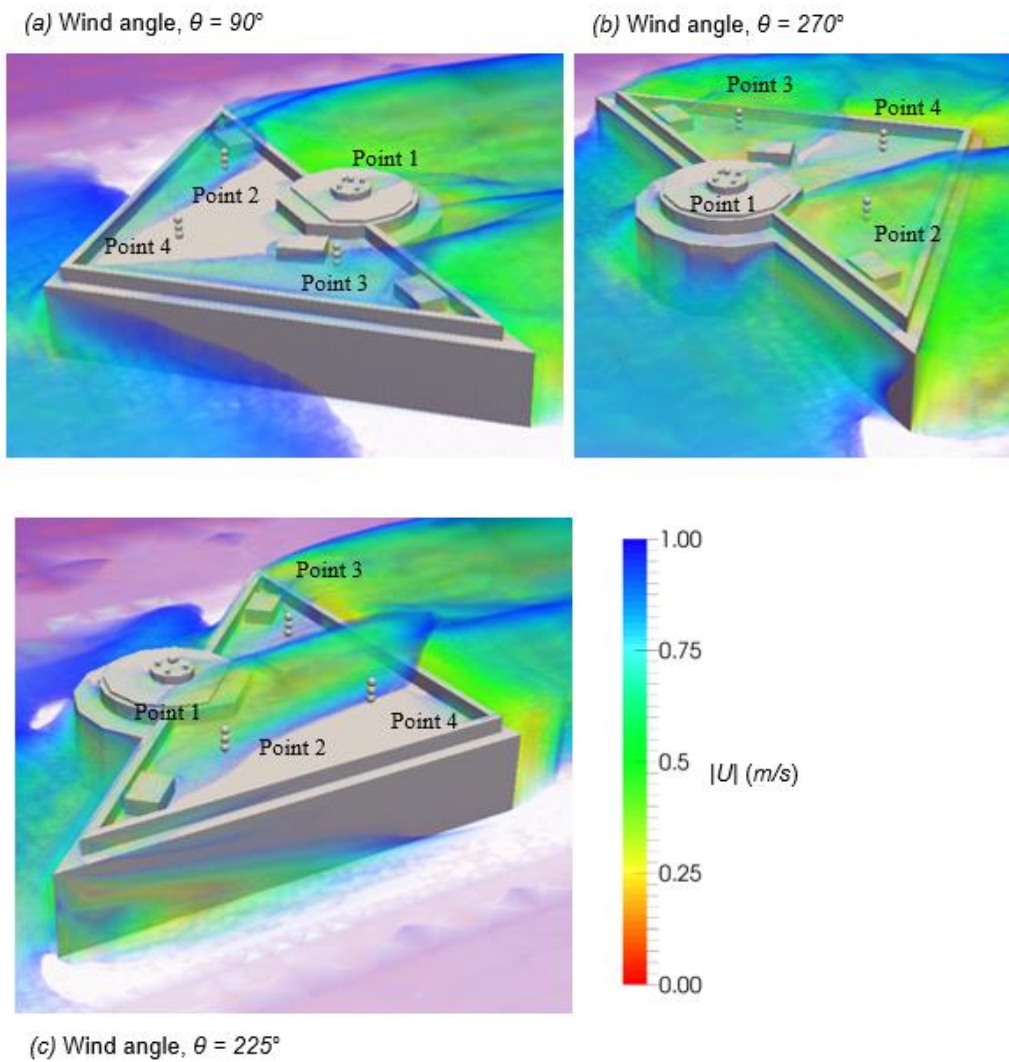


Figure 3: Volume rendering of the velocity magnitude $|U|$ for $|U| < 1 \text{ m/s}$ for wind angles (a) 90° , (b) 270° and (c) 225° . The bubble region highlights the region where the wind speed is insufficient to sustain the rotation of a typical vertical axis wind turbine.

Wall-normal Height	Location	Min. Wind Speed (m/s)	Max. Wind Speed (m/s)	Wind Mean Speed (m/s)	Standard Deviation	No. of Wind Directions Below Mean	No. of Wind Directions Below 0.5m/s
$z = 23\text{m}$	Point 1	-	-	-	-	-	-
	Point 2	0.17	1.70	1.01	0.59	3	2
	Point 3	0.10	1.66	0.99	0.55	4	1
	Point 4	0.31	2.01	0.93	0.62	6	2
$z = 25\text{m}$	Point 1	-	-	-	-	-	-
	Point 2	0.16	1.77	1.12	0.64	3	2
	Point 3	0.38	1.79	1.21	0.50	5	1
	Point 4	0.66	2.05	1.05	0.55	6	0
$z = 27\text{m}$	Point 1	1.10	2.38	1.80	0.46	2	0
	Point 2	0.68	1.89	1.50	0.44	4	0
	Point 3	0.87	1.90	1.57	0.35	3	0
	Point 4	0.80	2.06	1.36	0.43	6	0

Table 1: Summary of the horizontal wind speed results for the 4 locations at heights $z = 23\text{m}$, 25m and 27m .

Ideally, it would be best to place the wind sensors and the wind turbine as high as possible. However, having a pole which is higher than the lighting rod of the building significantly increases the risk of the devices being struck by lightning. This is an important consideration especially in Southeast Asian countries like Malaysia where there is a high occurrences of tropical thunderstorms. In addition, placing these devices at a high altitude would require fabricating a tall and sturdy support pole. It would be difficult to set up and maintain the devices. If the wind turbine is to be placed at $z = 27m$, the support pole needs to have a length of $8.34m$ if placed at points 2, 3 or 4 but only requires a length of $1.98m$ if placed at point 1 due to the higher elevation of the surface. Therefore, it would be favourable to place the wind sensors and wind turbine at point 1 as a significantly shorter support pole is needed.

4. Conclusion

The flow over UNITEN's administrative building is simulated using steady-state RANS. A total of 8 cases were conducted to provide a comprehensive prediction of the flow at different wind angles. The horizontal wind velocity magnitude at the roof of the building was analysed at four different roof locations at heights $z = 23m, 25m$ and $27m$. Results for the analysis conducted found that the optimal location to place the wind devices and wind turbine would be at point 1 at a height of $27m$. At this location and height, maximum mean wind speed is obtained and this location also has the highest minimum and maximum wind speed. In addition, the support pole required to fix the devices only has to be $1.98m$ high as point 1 is located at a higher elevation from the other points. This would make the assembly, installation and maintenance of the devices much easier.

5. Acknowledgements

This work was financially supported by Universiti Tenaga Nasional Internal Grant, under the green campus initiative project.

References

- [1] Government of Malaysia. *Intended Nationally Determined Contribution of the Government of Malaysia. 2016*. [Online]. Available: <http://www4.unfccc.int/submissions/INDC7>, no. 6, pp. 507–518, 2003.
- [5] I. Abohela, N. Hamza, and S. Dudek. Effect of roof shape, wind direction, building height and urban configuration on the energy yield and positioning of roof mounted wind turbines. *Renew. Energy*. 2013. 50: 1106–1118.
- [6] F. Toja-Silva, C. Peralta, O. Lopez-Garcia, J. Navarro, and I. Cruz. Roof region dependent wind potential assessment with different RANS turbulence models. *J. Wind Eng. Ind. Aerodyn.* 2015; 142: 258–271.
- [7] A. Kalmikov, G. Dupont, K. Dykes, and C. Chan. *Wind power resource assessment in complex urban environments: MIT campus case-study using CFD Analysis*. in AWEA 2010 Windpower Conference. Dallas, USA, 2010.
- [8] J. T. Millward-Hopkins, A. S. Tomlin, L. Ma, D. B. Ingham, and M. Pourkashanian. Assessing the potential of urban wind energy in a major UK city using an analytical model. *Renew. Energy*. 2013; 60:701–710.
- [9] H. G. Weller, G. Tabor, H. Jasak, and C. Fureby. A tensorial approach to computational continuum mechanics using object-oriented techniques. *Comput. Phys.* 1998; 12(6); 620–631.